Under-Vehicle Inspection Utilizing a Mobile Robot with a LRF Sensor

Sanngoen Wanayuth, Taichi Yamada, Akihisa Ohya and Takashi Tsubouchi

Abstract— **The under-vehicle inspection systems have led to an increased interest to develop the technologies for finding threats such as bomb, transmitter, and so on. In this paper, we presented the automated under-vehicle inspection in parking place utilizing a mobile robot. To obtain the underside of vehicle, laser range finder (LRF) is used to acquire data of object with directly measure under vehicle. Features of the approach include the method for under vehicle detection, pose estimation function, data alignment using iterative closest point (ICP algorithm), underside vehicle data comparison to find the differences between previously archived state and current state. Average height and detected size of the object were determined by item identification method. This strategy is presented to inspect and recognize underside of the vehicle change. Our approach has successfully shown to detect the object of under vehicle state changes. Experiments are conducted to demonstrate the efficiency of our approach to inspect and recognize objects under vehicles.**

I. INTRODUCTION

Automated an under vehicle inspection system is required for security and safeguard area from dangerous material or contraband item (e.g. explosives or other types of threats) that desired any parking place. The inspection station check point that much be examined vehicle undercarriage, the simply technique by using the convex mirror. The convex mirror technique does not work effectively in coverage entire undercarriage because the areas unviewed (occlusion caused by wheels), viewing angle (physical constraints on mirror), low lighting conditions, and it is difficult to operate a completely underside inspection of vehicle undercarriage. Other solution has been devised that uses a vision system installed onto an inspection bay built into the ground [1] for detecting underside of the vehicle by the vehicle is moving over its. Under condition, vehicle at lower speed and correctly direction of steering are necessary, hardware configuration for setting up with fix sizes and wider area are required. These above methods had been accomplished at the inspection check point of entrance gate such those as airports, embassies, federal buildings and so on.

In parking lots, the other threats were occurred such as car brake-in, car stolen, even risk as the dangerous item is appearing underside of vehicle. Many researches were developed mobile robot platform that employed for vehicle inspection tasks, to operate the underside of vehicle with sensors device for inspecting under vehicle. The mobile robots were implemented design with omni-direction wheel types, ODIS [2], Safebot [3], for robot motion underside of vehicle to inspect of vehicle undercarriage. The commonly vision sensor was installed on a mobile robot with visual image for viewing the vehicle undercarriage scene to the operator via wireless communication module. Functional features were proposed various methods for under vehicle inspection, for scene inspection by generate the mosaics [1] and multi-perspective mosaics image [4], [5] that have been deployed with the near-infrared camera and threat object detection using thermal camera [6]. The advantage of above sensor device could be viewed at all brightness and even in darkness. The field of view of camera was somewhat limited and a high performance processor was employed for computing vehicle undercarriage scenes. Moreover, 3D CAD model was generated of surface shape description of 3D data from under vehicle scene algorithm [7], [8] with laser scan combined the camera in RANGER system for created 3D geometry of a vehicle's undercarriage for better visualization. Recently, the Autonomous Solutions Inc., company was developed a compact size of mobile robot called "Spector" [9] that installed the pan/tilt camera module for monitoring underside of vehicle to operator via radio frequency communication system. For personnel identify contraband items such as weapons, bombs, and other security threats by viewing at monitor display. However, under vehicle inspection is once an important mission for preventing from threats e.g. items contraband, object explode, etc. The way out for detecting underside of vehicle, a mobile robot is applied to instead of human operation that mounted the sensor equipment to obtain data of vehicle undercarriage. In this paper, we proposed a small mobile robot to patrol in parking lots for under vehicle inspection with laser range finder (LRF) sensor. The LRF directly measures (distance, orientation) in wide range scanner and it is not effects in the lighting condition.

We have developed a system of parking lot inspection by using a mobile robot with LRF sensor for checking the vehicle as long term parked and empty lot checking [10]. Extending our previous work, in this paper we propose the approach for under vehicle inspection. The major contribution with our research is in enhancing existing inspection robot with 2D laser range sensor, to acquire geometric of a vehicle undercarriage and generated the 3D data, to define anomalous objects by comparing between previously achieved scan and current scan. In trying to provide such a robotic system as a reliable solution for under vehicle inspection, we enlist the following characteristics expected of an under vehicle inspection as follows; 1) obtain under vehicle data, 2) extract anomalous objects from under

Sanngoen Wanayuth, Taichi Yamada, Akihisa Ohya and Takashi Tsubouchi are with the Intelligent Robot Laboratory, Graduate School of Systems and Information Engineering, University of Tsukuba, 1-1-1 Tennodai, Tsukuba 305-8573, Japan. email: {wanayuth, tyamada, ohya, tsubo}@roboken.esys.tsukuba.ac.jp.

vehicle data, 3) identify anomalous objects on the current state.

Our proposed framework and automation procedures consider each one of the listed characteristics to inspect underside of the vehicle. In Section II, we briefly described the system architecture that takes care of data acquirement, motion planning, data alignment, data comparison of under vehicles, cluster anomalous objects from under vehicle data and object identification method. In section III, an overview of robot platform and LRF sensor are introduced. The experimental data are presented in section IV. Finally, the conclusions and future works are described in section V.

II. UNDER-VEHICLE INSPECTION SYSTEM

Our main research aims to inspect the under-vehicle state within parking lots, recognize object is appeared underside of the vehicle and object location at vehicle undercarriage utilizing a mobile robot with the LRF sensor. Two sensors are used for under vehicle detection and robot navigation. To acquire the geometric information underside from the target vehicle, the mobile robot moves underside of the vehicle (in Fig.1) to obtain under vehicle data. We purposed a mobile robot which performs to patrol with multiple time data scanners from starting point until cover underside of a vehicle and then go back to a target point. Under vehicle point cloud data is acquired by a LRF sensor. The multiple periods of time of scanned data (period of time stamps as t_1, t_2,..., t_n) for under vehicle detection is collected accordingly in this system. Consequently, data comparisons was done between scanned data from consecutive time frames between t_i and t_{i+1},... (where i = 1,2,...,n). These methods are described in this section.

A. Under-Vehicle Data Acquisition

The 2D plane of LRF provides the upright vertical plane scan that is perpendicular the ground to acquire under vehicle data as shown in Fig. 1. The 2D data range scan (angle and range) and self-positioning of the robot locomotion are combined to point cloud data in 3D world coordinates. The point cloud data from the LRF sensor consists of the under-vehicle data (U_j) and ground data.

For separating the point cloud data, the constant height value of $H_{threshold}$ along z axis is applied to divide the point cloud data. Point cloud data above $H_{threshold}$ are considered and other points below the threshold are ignored.

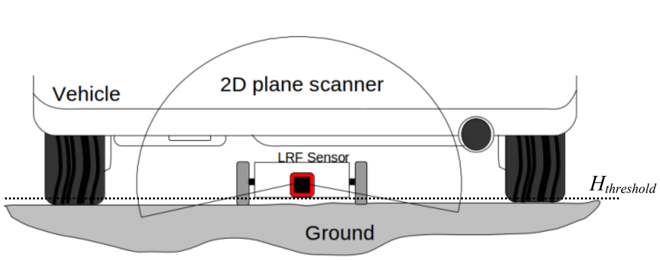

Fig. 1. 2D plane scanner of LRF for under-vehicle detection.

B. Motion Planning

Within under vehicle area, mobile robot moves underside of the vehicle to patrol whole under vehicle area. The 2D plane of laser range sensor provides horizontal plane (in Fig. 2) to detect tired wheels during robot navigation, to avoid colliding to those tires. Four tires can be used as the landmarks for robot localization relative to these tires. We provided the localization technique underside of a vehicle. The 2D range scan matching technique [11], [12] is applied to relative position tracking and localization. We proposed the path way of robot as U-curve (in Fig. 3) for motion planning whole under vehicle area from start point to target point.

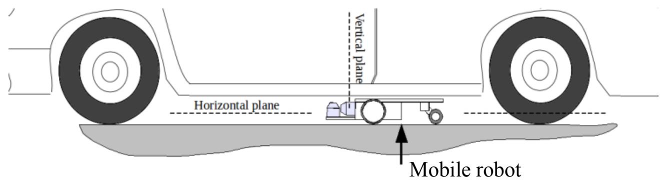

Fig. 2. Horizontal plane and vertical plane scan of LRF on a mobile robot.

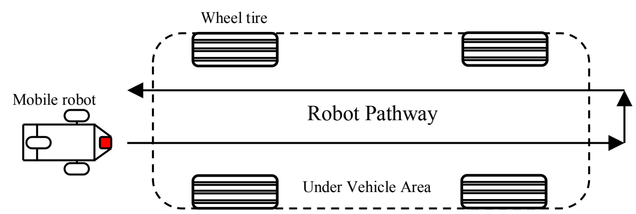

Fig. 3. Robot pathway of an under vehicle area

C. Under-Vehicle Data Alignment

In this section, the under-vehicle data from previously archived scan and current scan are used to compute under vehicle data alignment between them. The under vehicle data is related to robot position with odometry-base self-position, thus some coordinate error can occur while the robot collects information between multiple inspections. Therefore, we proposed data matching technique for data alignment. The ICP algorithm [13],[14] is applied for under vehicle data matching between base point cloud from previously archived scan and target point cloud from current scan.

With the data alignment method, the under-vehicle data is conducted for data alignment between base point cloud data ($U_j^{t_i}$) and target point cloud data ($U_j^{t_{i+1}}$) by a point pairs of under-vehicle data is calculated, where U is under vehicle data and t is multiple of duration time stamp. The method of computing the data alignment is described as follows:

a) Set base point data ($U_j^{t_i}$) and set target point data ($U_j^{t_{i+1}}$).

b) Pair each point of ($U_j^{t_i}$) to closest point in ($U_j^{t_{i+1}}$).

c) Compute transformation (R, T).

d) Apply motion to ($U_j^{t_i}$).

e) Repeat until data convergence is completed.

A concept is shown in Fig. 4, two under-vehicle data before data alignment is shown in Fig. 4(a). Under-vehicle data after data processing between them is shown in Fig. 4(b). With data alignment method, the transformation matrix (R, T) is computed to under vehicle data, where R is rotational matrix and T is translational matrix.

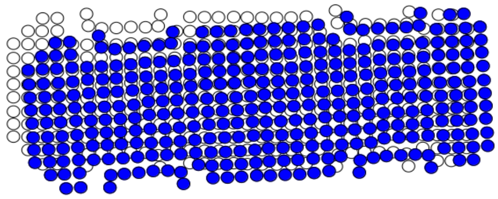

(a)

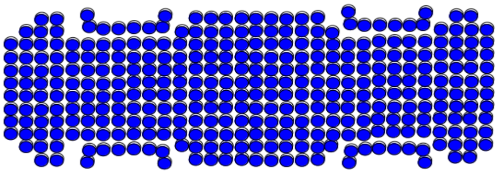

(b)

Fig. 4. Under vehicle data between previous scan and current scan in (a), after under-vehicle data alignment in (b).

D. Under-Vehicle Data Comparison

Within data comparison technique, under vehicle data (U_j) is used to compare from previous under vehicle data for detecting items underside of the vehicle such as an anomalous item is appearing on current state. In this section, to determine whether underside of the vehicle is status changes or same status by data comparison between previously archived scan and current scan. We mainly interested to inspect underside of vehicle, finding potential changes of vehicle undercarriage. The concept of under vehicle data on previously archived scan is shown in Fig. 5(a), the under vehicle data on current scan is shown in Fig. 5(b).

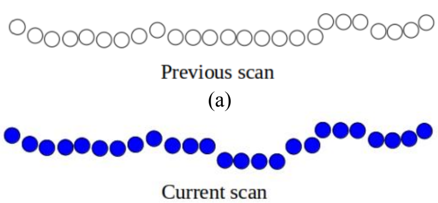

Fig. 5. Concept of under-vehicle data between previous archived scan (a) and current scan (b).

The data comparison approach processes all the data as follows: First, set under-vehicle data of base point cloud data $W_i \leftarrow U_j^{t_i}$, and target point cloud data $Q_j \leftarrow U_j^{t_{i+1}}$, where U is under-vehicle data, t is time duration of data scanner. Set $P_{threshold}$ is constant distance value. Second, searching the closet points by determine the distance (d) of point pairs from $d(\vec{Q},\vec{W})$ by using Euclidean distance in equation (1).

$$d(\vec{Q},\vec{W}) = |\vec{Q}_j,\vec{W}_i| = \sqrt{(x_i - x_j)^2 + (y_i - y_j)^2 + (z_i - z_j)^2} \quad (1)$$

To calculate the distance *(d)*, if d is less than a constant value $P_{threshold}$, the point data is ignored. If distance *(d)* is greater than a constant value $P_{threshold}$ the point data will be collected in set M_k as different point data. A concept is shown in Fig. 6, under-vehicle data of current scan with difference point data M_k as shown in Fig. 6(b). Finally, additional calculation is done to determine distance (d) of point pairs from $d(\vec{W},\vec{Q})$. The different point data is collected in set N_k as shown in Fig. 6(a). In case of under vehicles within the same state information or under vehicle state is no state change, the different point data is near zero.

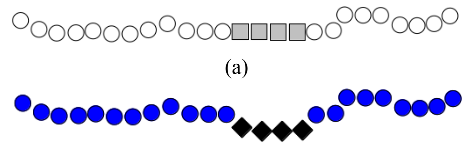

(a)

(b)

Fig. 6. Difference point data M_k in current scan (diamond points) in (b) and the difference point data N_k in previous scan (square points) in (a).

E. Data Segmentation and Identification

In this section, the point data M_k is used to calculate the item location and item identification as different state of vehicle undercarriage. To define item identification, clustering point data of M_k is performed to determine group of item, dimension size, and item location. The method of data segmentation based on the Euclidean distance (with noise being removed) and data identification method are proposed to define data specification. This solution is described as follow:

First, the distance (d) of point pairs is calculated. If the distance (d) value is less than threshold $S_{threshold}$, the point pair data will be collected and recorded in set $O_{q,b} \leftarrow M_k$. A new group of data is being created for the rest of point pair data and recorded in $O_{q,b+1} \leftarrow M_k$ where q is number of points in each group, b is group number.

Second, if the number of point in each group $O_{q,b}$ is less than the threshold $N_{threshold}$ value, that particular group will be removed where $N_{threshold}$ is set number of point. Finally, for each remaining groups, two sets are calculated, a 3D dimensional size (*width* × *length* × *height*) of data point and an average of height along the z-axis from ground. The technique is shown in Fig. 7. To check the status of object underside of the vehicle, an average height along z axis of object is used to compare between previous and current states. If average height of previous state is lower than an average height of current state, so the related object is appearing otherwise the object is missing.

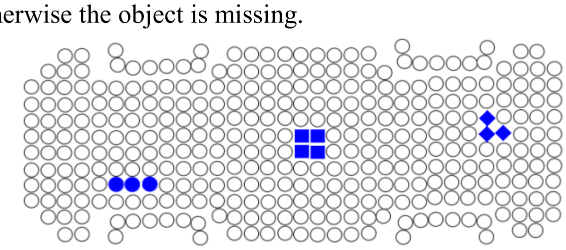

Fig. 7. Data segmentation of the different data points

III. HARDWARE

In Fig. 8, the compact size robot platform is developed for this study. The robot size is W0.32×H0.11×L0.52 (width×height×length, unit *m* is meter) with SOKUIKI sensors (UTM-30LX, Hokuyo Automatic Co., Ltd.) as laser range finder (LRF) sensors. Two LRF sensors are installed on robot platform for data measurement of the vehicle undercarriage and robot localization. A sensor is installed upright vertical plane that perpendicular on the ground plane in order to acquire geometric information under the vehicle and a sensor is installed in front of robot in horizontal plane (parallel to ground) to perform the robot localization function. The sensor is a compact size (W60×D60×H87 *mm*), cover detection range about 0.1 to 30 *m*, distance accuracy is 0.03 *m*, angular resolution is 0.25 degrees, and angle range is 270 degrees operating at 40 Hz.

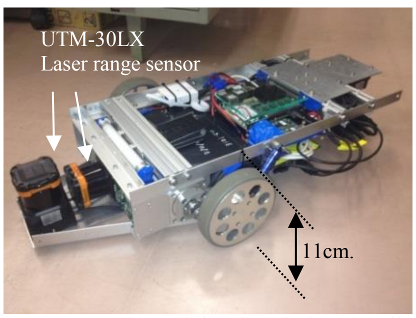

Fig. 8. A compact size mobile robot platform is called “SIZKA”.

In Fig. 9, a main processor used is Intel 1.6 GHz 2GB RAM based small-size PC board running Ubantu12 distribution of Linux (kernel 3.2.0-36-generic-pae) as operating system. The dimension of small-size PC board is W0.1×H0.034×L0.122 (unit *m* is meter). The robot controller board with SH2 processor provides robot locomotion and odometry-based self-position estimation function. The wireless communication module (IEEE802.11b/g/n, 150 Mbps) is applied for data communication between robot and operator as enable manual mode in order to control the robot.

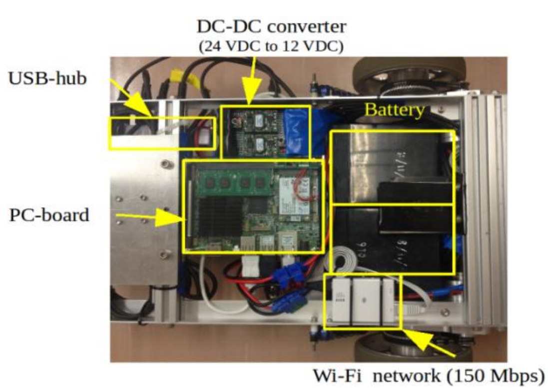

Fig. 9. Hardware component on robot platform.

IV. EXPERIMENTAL RESULTS

In the experiments, a mobile robot velocity is 0.15 m/sec for robot movement underside of the vehicle. A mobile robot is moved under vehicle to obtain under vehicle data that operate to data scanner underside of the vehicle in multiple period time duration ($t_1, t_2, \ldots, t_n$). For the experiments at least two time stamp of data from mobile robot operation is required with the same a parking lot and same vehicle also. The data from sensor was read every 25 *ms* by a driver process, registered in parallel into a shared memory system (SSM) [15], and was recorded in data log file.

For motion planning as *U*-curve, a robot moved forward direction from start point, a maximum distance at 4.5 meter over range of under vehicle area and then rotated at 90 degree, and moved forward at 0.5 meter and then rotated back for moving to target point. In the experiment, the robot motion with odometry-base function is generated positioning error of robot while robot operational. The measurement error is less than 0.45 meter at target point. We applied the scan matching technique to align between data range scanners and robot position estimation. The measurement error is less than 0.1 meter at target point. The obstacle avoidance technique is not employed in this paper. The result is shown in Fig 10.

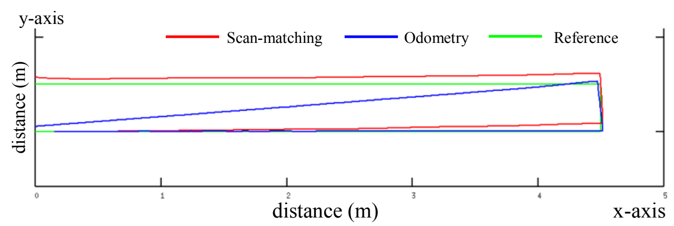

Fig. 10. Set a path planning (green line), robot motion with odometry estimation (blue line) and localization (red line).

As the result of robot motion, the under vehicle data is collected the position of under vehicle while robot operational. In Fig. 11, the under vehicle data is collected from robot motion with robot odometry-base estimation function, so the point data is overlapped.

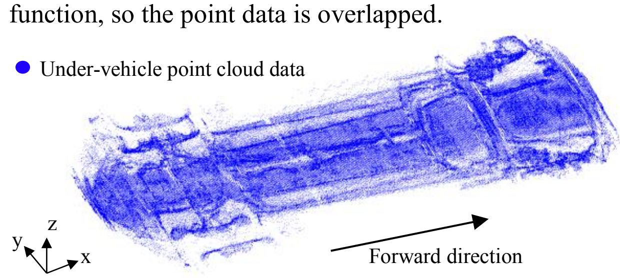

Fig. 11. Under-vehicle point cloud data is overlapped with the odometry-base function.

In Fig. 12, under vehicle data is collected the position of under vehicle to relate pose estimation of robot. Under vehicle data is aligned the position of under vehicle while collected point data by robot localization function. Therefore, function of robot localization is applied for all experiments. The height distance along z axis of under vehicle data is shown in Fig.13. The ground point cloud data included in experiment data, for removing the ground data by setting of $H_{threshold}$ at 0.02 *m*. point cloud data below $H_{threshold}$ is removed.

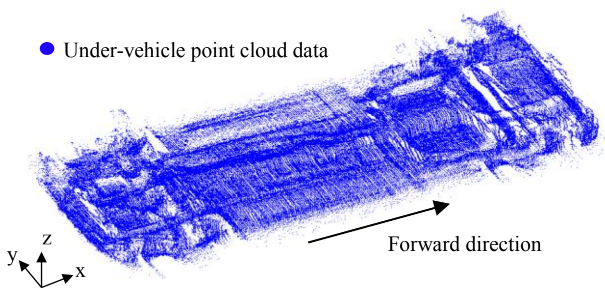

Fig. 12. Under-vehicle point cloud data is collected with localization function.

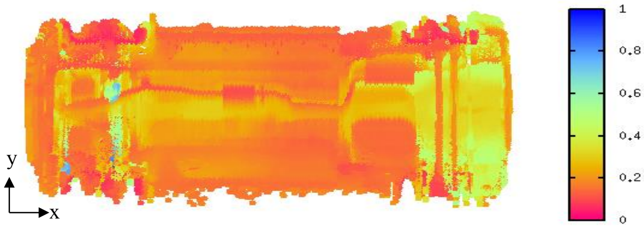

Fig. 13. Image of under-vehicle data with the height distance along z-axis (color bar unit: *m* is meter)

The result of the under vehicle data detection is being processed to obtain under vehicle data alignment from the previous inspection and current one as shown in Fig. 14(a). In this experiment, the under vehicle data alignment between them is then calculated using transformation matrix (R,T) which applied to under vehicle data. This method is shown in Fig. 14(b). From under vehicle data alignment, under vehicle data is calculated by transformation matrix. To check under vehicle state changes, under vehicle data is obtained for calculating the distance of point pairs between previously archived scan and current scan by data comparison method.

The constant value $P_{threshold}$ is set at 0.02 *m*. and applied to all of experiments. From the experimental result of data comparison, in case of state changes, data points are grouped by data segmentation method. Euclidean distance with the threshold distance of $P_{threshold}$ is the key to group the above data. For each group, if number of point is greater than threshold value of $N_{threshold}$, the point data from group is collected. A number of point $N_{threshold}$ is set at 100 point by defined a threshold value from the minimum of point of each group. A threshold $N_{threshold}$ is applied to all the experiments. Finally, item identification method is applied to calculate an average of height distance along z axis and dimension size ($W \times L \times H$), where W is width range along x axis, L is length range along y axis and H is height range along z axis. In experiments, the box and cylinder shape of items are used as threat objects (such as dynamite, plastic bomb). The experiments of method approach are presented in Fig. 15 and Fig. 16 in order to inspect threat objects underside of the vehicle. Threat object could not detected in Fig. 17. The detected size of item is summarized in Table 1.

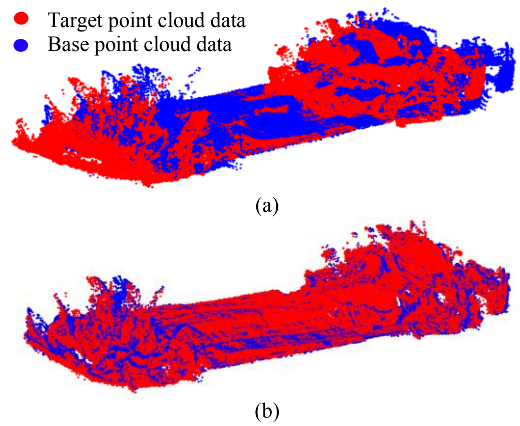

Fig. 14. Under-vehicle data from previous scan and current scan in (a), after data alignment in (b).

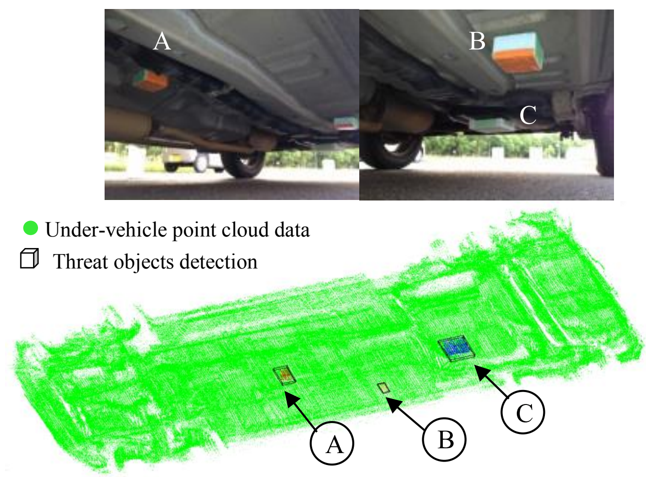

Fig. 15. Threat objects (three items) are appearing in current state and threat object detection.

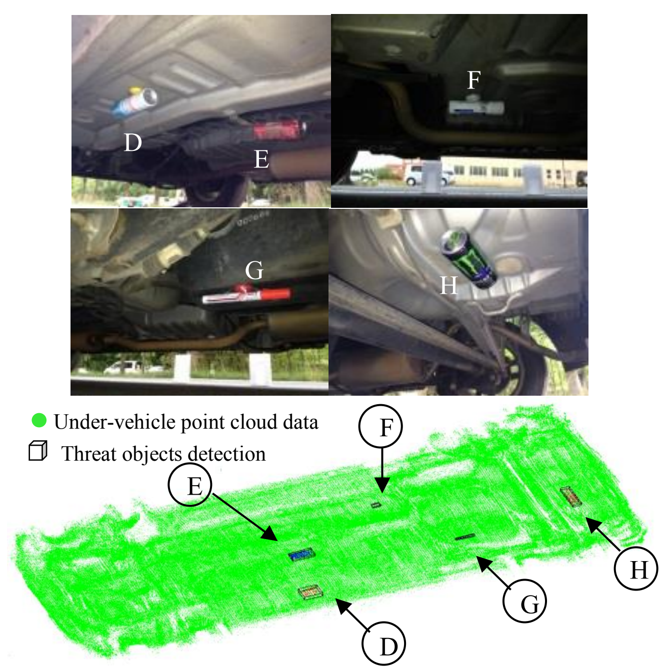

Fig. 16. Threat objects (five items) are appearing in current state and threat object detection.

TABLE I

The average height distance of under vehicle data inspection (unit: *m* is meter).

Items	Detected size (*m*) ($W \times L \times H$)	Average height (*m*)		Item height (*m*)
		Previous	Current	
A	0.07×0.15×0.03	0.11	**0.17**	0.031
B	0.04×0.08×0.02	0.07	**0.12**	0.025
C	0.14×0.06×0.04	0.03	**0.09**	0.041
D	0.10×0.09×0.10	0.11	**0.16**	0.101
E	0.13×0.06×0.05	0.12	**0.17**	0.058
F	0.66×0.03×0.02	0.09	**0.12**	0.026
G	0.11×0.017×0.02	0.08	**0.10**	**0.021**
H	0.06×0.12×0.07	0.21	**0.27**	0.064

In experimental results, the minimum height 0.021 meter of the item can be detected by this method. The item height is calculated by data range from maximum and minimum points along z axis. An item as a mobile phone whose height is 0.015 meter could not be detected as shown in Fig. 17.

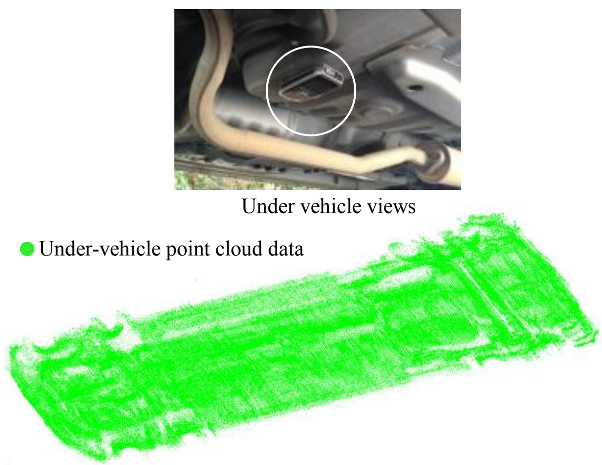

Fig. 17. Threat object (mobile phone) is appearing in current state and the proposed methods cannot detected.

In condition item appearing is declared if an average of height distance value of current state is greater than an average of height distance value of previous state. In this paper, the application of under vehicle inspection is proposed for checking under vehicle state changes. From the experiments, the proposed method could locate and identify the threat object is appearing on current state. However, in case of repeated processes on the same vehicle, if the value of average height is near zero then there is no state change of underside of the vehicle.

V. Conclusion and Future work

Our implementation has demonstrated the functional feature for underside of vehicle inspection system within a parking lot, which achieved the practical use a LRF sensor utilizing a mobile robot in real environment. By multiple time of data scanner of patrol robot was introduced in this work. The ability of LRF was introduced to acquire the geometry of a vehicle's undercarriage. By a small mobile robot was developed to exam under vehicle area with the localization function and object identification function. In this work, the proposed application was applied to protect underside of vehicle from threats in parking lots for automated an under vehicle inspection system.

As future works, sensors (e.g. thermal camera, IR camera, radiation sensor, etc.) will be installed to increase performance of inspection and identification from threat objects underside of vehicle. The function of license plate number inspection will be developed to recognize the vehicle in parking lot and also the navigation system will be developed to patrol in parking lots.

References

[1] P. Dickson, J. Li, Zhu. Zhigang, A.R. Hanson, E.M. Riseman, H. Sabrin, H. Schultz, and G. Whitten, "Mosaic Generation for Under Vehicle Inspection," *Proc. 6th IEEE workshop on Applications of Computer Vision (WACV)*, Orlando, FL, USA, pp. 251-256, 2002.

[2] N.S. Flann, K.L. Moore, and L. Ma, "A small mobile robot for security and inspection operations," *Journal of Control Engineering Practice*, Vol. 10, No. 11, November 2002 , pp. 1265-1270(6)

[3] C.Qian, D. Page, A Koschan, and M. Abidi, "A 'Brick'–Architecture -Based Mobile Under-Vehicle Inspection System," *Proc. of the SPIE Unmanned Ground Vehicle Technology VII*, Vol. 5804, pp. 182-190, March 2005.

[4] B. Ramadoss, J.-C. Ng, A. Koschan, and M. Abidi, "Scene Inspection Using Robotic Imaging System," *Proc. of SPIE 6th International Conference on Quality Control by Artificial Vision*, Vol. 5132, pp. 323-330, Gatlinburg, TN, May 2003.

[5] A. Koschan, J.-C. Ng, and M. Abidi, "Multi-perspective Mosaics for Under Vehicle Inspection," *Proc. SPIE Unmanned Ground Vehicle Technology VI*, vol. 5422, Orlando, FL, USA, pp. 1-10, April 2004.

[6] S. Sukumar, D. Page, A. Gribok, A. Koschan, M. Abidi, D. Gorsich, and G. Gerhart, "Surface Shape Description of 3D Data from Under Vehicle Inspection Robot," *Proc. SPIE Unmanned Ground Vehicle Technology VII,* Vol. 5804, Orlando, FL, pp. 621-629, March 2005.

[7] C.Chung-Hao, C. Chang, P.David, K. Andreas, A. Mongi, "Modular robotics and intelligent imaging for unmanned systems", *Proc. of SPIE Unmanned Systems Technology VIII,* Vol. 6230, pp. 43-52, April 2006.

[8] S.R. Sukumar, D.L. Page, A.V. Gribok, A.F. Koschan, M.A. Abidi, D.J. Gorsich, and G.R. Gerhart, "A Robotic 3D Imaging System for Under Vehicle Inspection," *Journal of Electronic Imaging*, Vol. 15, No. 3, 033008, 2006.

[9] Autonomous Solutions Inc., "Spector: Under vehicle inspection system", Product Brochure, 2005.

[10] S. Wanayuth, A. Ohya, and T. Tsubouchi, "Parking Place Inspection System Utilizing a Mobile Robot with a Laser Range Finder," IEEE/SICE International Symposium on System Integration, Kyushu University, Fukuoka, Japan, Dec. 16-18, 2012.

[11] B. Peter and S. Wolfgang, "The Normal Distributions Transforms: A New Approach to Laser Scan Matching," Proceedings of the 2003 IEEE/RSJ International Conference on Intelligent Robots and Systems, pp. 2743-2748, 2003.

[12] E. Takeuchi and T. Tsubouchi, "A 3-D Scan Matching using Improved 3-D Normal Distributions Transform for Mobile Robotic Mapping," Proceedings of the 2006 IEEE/RSJ International Conference on Intelligent Robots and Systems, pp. 3068-3073, 2006.

[13] N. Andreas, "Parallel and Cashed Scan Matching for Robotic 3D Mapping," *Journal of Computing and Information Technology*, pp. 51-65, 2009.

[14] A. Segal, D. Haehnel, and S. Thrun, "Generalized-icp," in Proceedings of Robotics: Science and Systems, Seattle, USA, June 2009.

[15] E. Takeuchi, T. Tsubouchi, and S. Yuta, "Intergration and Synchronization of External Sensor Data for a Mobile Robot," *SICE Annual Conference in Fukui,* August 4-6 2003, Fukui University, Japan.